



## 1,1-Dimethylbiguanide-Functionalized Magnetic Mesoporous Silica for Magnetic Removal of Cu<sup>2+</sup> from water

M. Beygzadeh

Department of Energy,

Materials and Energy Research Center, Alborz, Iran

(Corresponding author: M. Beygzadeh, m\_beygzadeh@yahoo.com)

(Received 24 April, 2016, Accepted 05 June 2016)

(Published by Research Trend, Website: www.researchtrend.net)

**ABSTRACT:** A 1,1-Dimethylbiguanide-functionalized magnetic mesoporous silica material (called Fe<sub>3</sub>O<sub>4</sub>/mSiO<sub>2</sub>-Met), was synthesized and determining its efficiency in copper removal from aqueous solutions with the study the effect of pH, contact time, initial concentration of Cu (II) ions and adsorbent dosage in a batch system was investigated. The materials were characterized by X-ray diffraction, TEM, Fe-SEM, N<sub>2</sub> adsorption-desorption (BET and BJH), VSM, and FT-IR. The experimental data were analyzed using the Langmuir and Freundlich models of adsorption. The results showed that the adsorption of Cu ions by adsorbent were suitable for Freundlich adsorption isotherm. Adsorbent could be efficiently separated by an external magnetic field from the reaction medium. Furthermore, results showed that adsorbent could be regenerated using HNO<sub>3</sub> 1 M and used for 4 sequential cycles of adsorption/desorption experiments, without significant loss of removal efficiency.

**Keywords:** Adsorption, Magnetic mesoporous silica, Biguanide, Copper removal, Freundlich isotherm

### INTRODUCTION

Toxic heavy metals such as Cu(II), Pb(II) and Cd(II) in liquid effluents have been caused as a result of an exponential increase in the use of heavy metals in industrial processes and products. Exposure to elevated levels of heavy metals can directly cause various adverse health effects to humans by impairing mental and neurological functions (Järup 2003, Ngah *et al.*, 2004, Atia *et al.*, 2005, Chang *et al.*, 2006). Some general techniques for heavy metals removal are precipitation, ion exchange (Vilensky *et al.*, 2002, Plazinski and Rudzinski 2009), reverse osmosis, membrane separation and adsorption (Yu *et al.*, 2000, Hasan *et al.*, 2009). Among them, adsorption is the most promising and frequently used technique owing to its convenient application and superior efficiency (Demirbas 2008, Ngah *et al.*, 2011).

Mesoporous materials, having large surface area and, high pore volumes, have been extensively studied for its broad applications in many areas, such as catalysis, sensors, controlled-release delivery system, and separation (Kresge *et al.*, 1992, Giri *et al.*, 2005, Alizadeh *et al.*, 2012a, Ahmadi *et al.*, 2014). Magnetic iron oxides such as magnetite (Fe<sub>3</sub>O<sub>4</sub>) and maghemite (-Fe<sub>2</sub>O<sub>3</sub>) have been investigated intensively for environmental and bio-applications. Fe<sub>3</sub>O<sub>4</sub>

nanoparticles embedded in mesoporous materials is of great interest for the development of high quality adsorbents combined with convenient separation using an external permanent magnet (De *et al.*, 2008, Liu *et al.*, 2008, Li *et al.*, 2011, Beygzadeh *et al.*, 2013).

In order to obtain specific adsorption and larger capacity, modification with ligand, such as amines, carbonates and organo sulfides on the surface of mesoporous materials is necessary (Burleigh *et al.*, 2001, Liu, *et al.* 2008, Sepehrian *et al.*, 2009, Wang *et al.* 2010). Besides having two imine groups in cis position, the biguanide group is an excellent ligand to give highly colored chelate complexes of the transition series, especially copper (II), nickel (II), cobalt (II) and platinum(II) (Ray 1961, Zhu *et al.*, 2002, Ansari *et al.*, 2010).

In previous our papers, we have synthesized a novel biguanide-functionalized Fe<sub>3</sub>O<sub>4</sub>/SiO<sub>2</sub> magnetite nanoparticle with a core-shell structure for utilization as a heterogeneous catalyst and nano-enhanced membranes in water treatment (Alizadeh, *et al.* 2012a, Beygzadeh, *et al.* 2013, Ghaemi, *et al.* 2015). In continuing of this study, a novel magnetic mesoporous silica adsorbent functionalized with 1,1-Dimethylbiguanide (Fe<sub>3</sub>O<sub>4</sub>/mSiO<sub>2</sub>-Met) was developed and used for copper ions removal.

## MATERIAL AND METHODS

### A. Chemicals and characterization

FeCl<sub>2</sub>·4H<sub>2</sub>O, FeCl<sub>3</sub>·6H<sub>2</sub>O, ammonium hydroxide (28% NH<sub>3</sub> in water), tetraethylorthosilicate (TEOS), 3-chloropropyl-trimethoxysilane (CPTS) and solvents were purchased all from Merck. IR spectra were determined on a Bruker V33 instrument. X-ray powder diffraction patterns were obtained on X'pert MPD Philips DW371. The specific surface area (BET method), the total pore volume and the mean pore diameter (BJH method) were measured using a N<sub>2</sub> adsorption-desorption isotherm by using a Belsorp-Mini II, Gemini 2375 (Bel Japan Inc.).

**Synthesis of Fe<sub>3</sub>O<sub>4</sub>/mSiO<sub>2</sub>.** First, Fe<sub>3</sub>O<sub>4</sub> magnetic fluid (about 2.0 wt%) was prepared according to previously reported (Alizadeh *et al.*, 2012b). Following the Stöber method with some modifications, 2 mL of above magnetic fluid, 20 mL of H<sub>2</sub>O and 1.5 mL of ammonia aqueous solution (28%) with ultrasonication for 20 min were poured into 60 mL of ethanol with vigorous stirring at 40°C. In the following, 20 mL of tetraethylorthosilicate (TEOS) ethanol solution (TEOS 0.3 mL) was added into the above mixture within 1 h using a dropping funnel. Three hours later, a 60 mL of mixed solution containing the cetyltrimethylammonium bromide (CTAB 0.36 g, 0.988 mmol) and polyvinylpyrrolidone (PVP K30 0.05 g) was rapidly transmitted into the above flask, and then 10 mL ethanol solution of TEOS (0.35 mL) was dropped into the flask within 0.5 h. After reaction for 3 h, the product was collected by magnetic separation and washed with ethanol and deionized water in sequence. In order to remove the template CTAB, the Fe<sub>3</sub>O<sub>4</sub>/mSiO<sub>2</sub> nanoparticles were refluxed in a mixture (30 mL of ethanol and 0.25 mL of 12 M concentrated HCl) at 40°C for 3 h, and then final obtained product was vacuum dried at 50°C.

**Synthesis of Fe<sub>3</sub>O<sub>4</sub>/mSiO<sub>2</sub>-Met.** First, a mixture of Fe<sub>3</sub>O<sub>4</sub>/mSiO<sub>2</sub> (1 g) and 1 mL (5 mmol) of CPTS in 100 mL in dried toluene was stirred for 18 h at 60°C. The obtained magnetic solid (Fe<sub>3</sub>O<sub>4</sub>/mSiO<sub>2</sub>-Cl) was separated by a magnet, washed with toluene and dried in vacuum. Then, the prepared Fe<sub>3</sub>O<sub>4</sub>/mSiO<sub>2</sub>-Cl (1 g) and KI (1.66 g, 10 mmol) were added to a solution of metformin hydrochloride (0.21 g, 5 mmol) and K<sub>2</sub>CO<sub>3</sub> (10 mmol, 1.38 g) in acetonitrile (50 mL) in a round-bottom flask and the mixture was stirred under reflux condition for 5 hrs. The obtained solid was then magnetically collected from the solution and washed copiously with water/ethanol followed by drying at 80°C for 6 hrs.

### B. Adsorption procedure

Adsorption isotherms of Cu(II), onto Fe<sub>3</sub>O<sub>4</sub>/mSiO<sub>2</sub>-Met nanoparticles were obtained from batch experiments by placing various amount of Fe<sub>3</sub>O<sub>4</sub>/mSiO<sub>2</sub>-Met in 50 ml cap polypropylene and metal ion solution 25 ml with varying concentrations of copper ions. All experiments was performed in 200 rpm stirring speed of stirrer at 20°C temperature. Fe<sub>3</sub>O<sub>4</sub>/mSiO<sub>2</sub>-Met nanoparticles were magnetically separated from the aqueous solution and the residual concentrations of metal ions in the aliquot were determined by atomic absorption spectroscopy (AAS) (Gbc 932 plus). The effect of pH on the adsorption of Cu(II) onto Fe<sub>3</sub>O<sub>4</sub>/mSiO<sub>2</sub>-Met was investigated using solution of different pH 2-8 at 20°C temperature. Metal solution at this pH was adjusted using 0.1N HNO<sub>3</sub> and 0.1 NaOH. The equilibrium-adsorbed concentration, q<sub>e</sub>, was calculated according to the equation:

$$q_e = \frac{(C_0 - C_e) \times V}{M}$$

where C<sub>0</sub> (mg/l) is the initial concentration of metal ion, C<sub>e</sub> (mg/L) is the equilibrium concentration in solution, V (L) is the total volume of solution, and M (g) is the sorbent mass. The percentage removal of Cu(II) ions from the solution was calculated using the following relationship:

$$R\% = \frac{(C_0 - C_e) \times 100}{C_0}$$

All the experiments were repeated three times, and the reported values represent the averages.

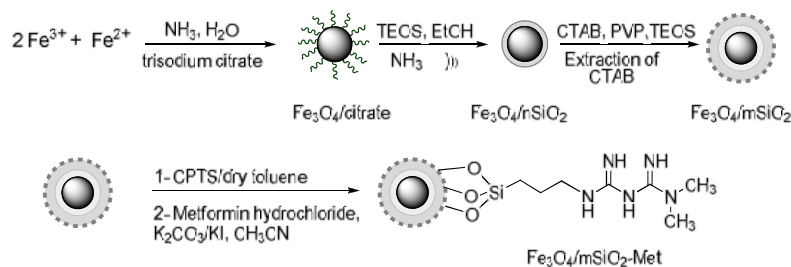
### C. Desorption and regeneration studies

To evaluate the reusability of the nanoadsorbent, adsorption of Cu(II) and regeneration of Cu-loaded Fe<sub>3</sub>O<sub>4</sub>/mSiO<sub>2</sub>-Met were performed in four consecutive cycles. In each cycle, 0.30 mg/L Cu(II) in 50 ml of solution was mixed with 35 mg Fe<sub>3</sub>O<sub>4</sub>/SiO<sub>2</sub>-Met for 2 h. The nanoadsorbent were separated magnetically and the supernatant was subjected to Cu(II) measurements. The resultant Cu-loaded sorbent was mixed with 10 ml of 1 mol/L HNO<sub>3</sub> solution for 30 min. Prior to the next adsorption desorption cycle, regenerated Fe<sub>3</sub>O<sub>4</sub>/mSiO<sub>2</sub>-Met were washed thoroughly with deionized water till pH = 6.

## RESULTS AND DISCUSSION

### A. Characterization of adsorbents (Fe<sub>3</sub>O<sub>4</sub>/mSiO<sub>2</sub>-Met)

Schematic steep of the reaction pathways and the resulting products 1,1-Dimethylbiguanide-functionalized magnetic mesoporous silica (Fe<sub>3</sub>O<sub>4</sub>/mSiO<sub>2</sub>-Met), are shown in Scheme 1.



**Scheme 1.** Schematic procedures shown for the preparation of ( $\text{Fe}_3\text{O}_4/\text{mSiO}_2\text{-Met}$ ).

The XRD pattern of the prepared  $\text{Fe}_3\text{O}_4$  and  $\text{Fe}_3\text{O}_4/\text{mSiO}_2\text{-Met}$  shown in Fig. 1. The pattern of the synthesized  $\text{Fe}_3\text{O}_4$  is compatible results reported in the literature. Considering Fig. 1(b), the presence of a broad peak at 20-28 confirms formation of silica layer without changing in the crystalline structure of the  $\text{Fe}_3\text{O}_4$  (Yang, Hu and Fu 2009).

The TEM images of the  $\text{Fe}_3\text{O}_4$  nanoparticles are shown in Fig. 2 (a), the average particle sizes of  $\text{Fe}_3\text{O}_4$  was observed to be 10 nm. Moreover, Fig. 2 (b) shows SEM microphotograph of  $\text{Fe}_3\text{O}_4/\text{mSiO}_2\text{-Met}$  nanoparticles, which proves the nanometric structure of particles. Nitrogen adsorption isotherms, BET surface area and pore volume of the synthesized  $\text{Fe}_3\text{O}_4/\text{mSiO}_2$  and  $\text{Fe}_3\text{O}_4/\text{mSiO}_2\text{-Met}$  assessed from  $\text{N}_2$  adsorption isotherm at 196°C are presented in (Fig. 3, Table 1). The illustrated isotherms for all materials were Type IV with a H1 hysteresis loop, which is typical for mesoporous materials with ordered pore structures.

After modification of  $\text{Fe}_3\text{O}_4/\text{mSiO}_2$  with biguanide, the BET surface area, Total pore volume were decreased due to presence of 1,1-Dimethylbiguanide ( $\text{Fe}_3\text{O}_4/\text{mSiO}_2\text{-Met}$ ).

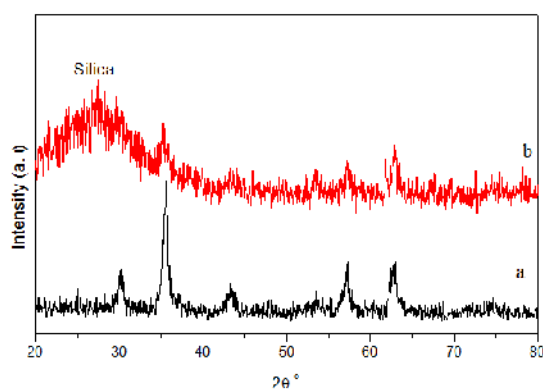


**Fig. 1.** Powder X-ray diffraction (XRD) patterns of (a)  $\text{Fe}_3\text{O}_4/\text{citrate}$ , (b)  $\text{Fe}_3\text{O}_4/\text{mSiO}_2$ .

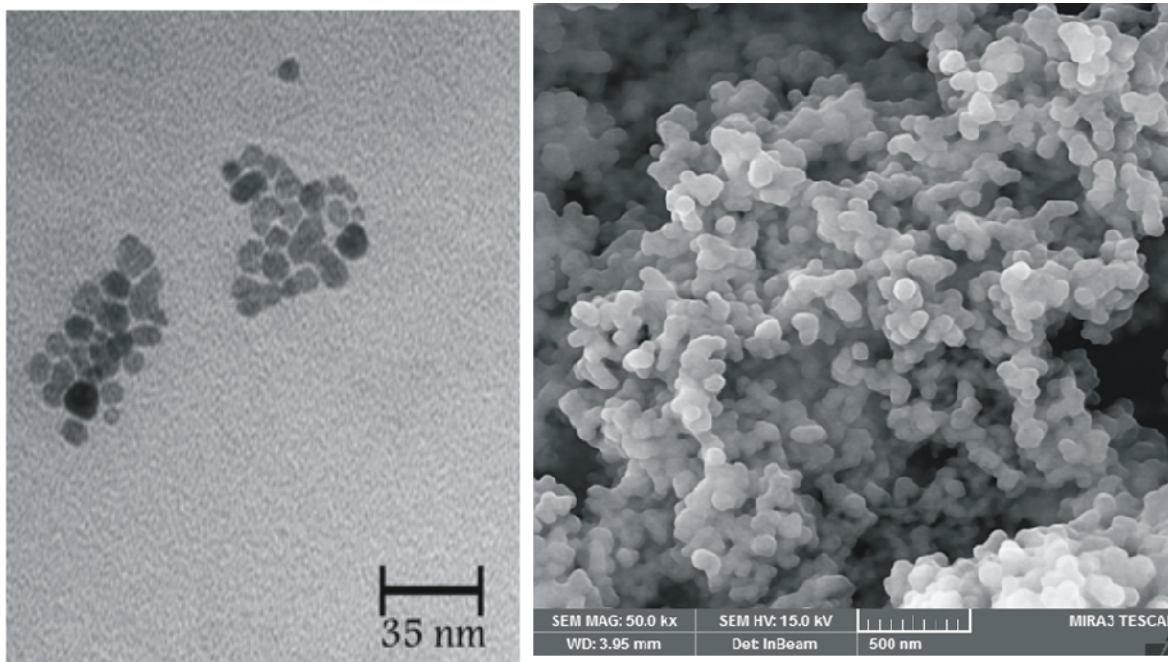


**Fig. 2** (a) TEM image of  $\text{Fe}_3\text{O}_4/\text{citrate}$  (b) Fe-SEM image of  $\text{Fe}_3\text{O}_4/\text{mSiO}_2\text{-Met}$ .

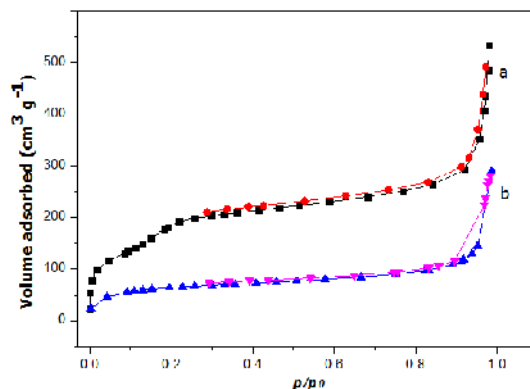


Fig. 3. N<sub>2</sub> adsorption-desorption isotherms of Fe<sub>3</sub>O<sub>4</sub>/mSiO<sub>2</sub> and Fe<sub>3</sub>O<sub>4</sub>/mSiO<sub>2</sub>-Met.

Table 1: The textural parameters of Fe<sub>3</sub>O<sub>4</sub>/mSiO<sub>2</sub> and Fe<sub>3</sub>O<sub>4</sub>/mSiO<sub>2</sub>-Met.

| Samples  | Mean pore diameter (nm) | S <sub>BET</sub> (m <sup>2</sup> g <sup>-1</sup> ) | Total pore volume (cm <sup>3</sup> g <sup>-1</sup> ) |
|--|-------------------------|--|--|
| Fe <sub>3</sub> O <sub>4</sub> /mSiO <sub>2</sub>      | 4.21                    | 781  | 0.824  |
| Fe <sub>3</sub> O <sub>4</sub> /mSiO <sub>2</sub> -Met | 7.78                    | 230  | 0.448  |

1,1-Dimethylbiguanide functionalization of Fe<sub>3</sub>O<sub>4</sub>/mSiO<sub>2</sub> nanoparticles can be confirmed by FT-IR spectra. Fig. 4(a) shows FT-IR spectrum of Fe<sub>3</sub>O<sub>4</sub>/mSiO<sub>2</sub>, the sharp band at 1090 cm<sup>-1</sup> is due to Si-O-Si antisymmetric stretching vibration, which proves the existence of a SiO<sub>2</sub> layer around Fe<sub>3</sub>O<sub>4</sub> nanoparticles. The observed peak at 1625 and 1475 cm<sup>-1</sup> in curves b are attributed to C=N and C-N stretching of metformin. Appearance of such bands is in a good agreement with the attachment of biguanide to the silica structure (Gunasekaran *et al.*, 2006).

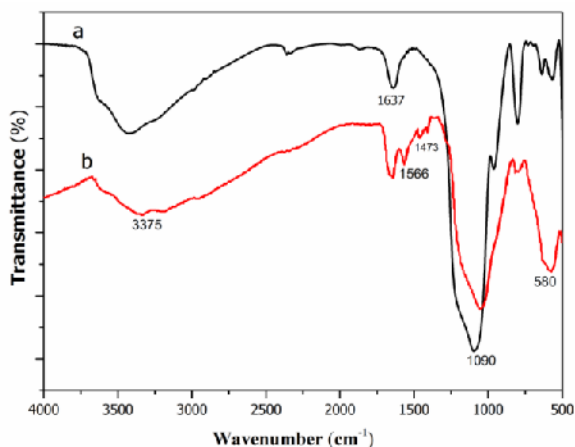


Fig. 4. FT-IR spectra of Fe<sub>3</sub>O<sub>4</sub>/mSiO<sub>2</sub> and Fe<sub>3</sub>O<sub>4</sub>/mSiO<sub>2</sub>-Met.

The magnetic property of Fe<sub>3</sub>O<sub>4</sub>/mSiO<sub>2</sub>-Met nanoparticle was characterized by a vibrating sample magnetometer (VSM) and Fig. 5 shows the typical room temperature magnetization. The M<sub>s</sub> of the Fe<sub>3</sub>O<sub>4</sub>/SiO<sub>2</sub>-Met nanocatalyst prepared in this study is 10 emu/g.

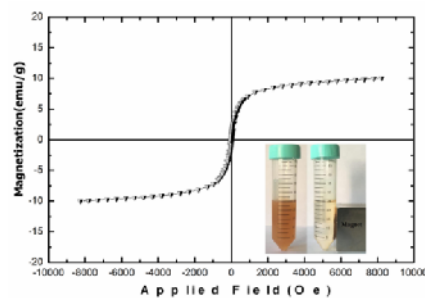
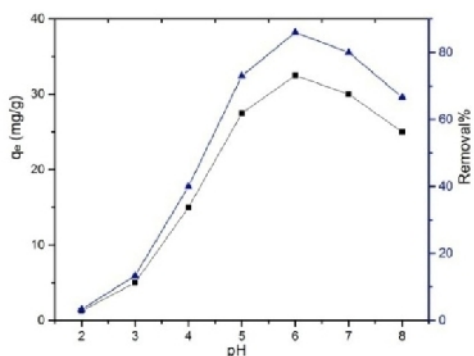


Fig. 5. Hysteresis loop of the Fe<sub>3</sub>O<sub>4</sub>/mSiO<sub>2</sub>-Met nanoparticle at room temperature, separation from suspension with an external magnetic field at 4 min (inset).

#### B. Adsorption studies

**Effect of pH.** The effect of pH on the adsorption of Cu(II) ions onto Fe<sub>3</sub>O<sub>4</sub>/mSiO<sub>2</sub>-Met was studied by mixing 20 mg of adsorbent with 25 ml of Cu(II) solution (30 mg/l) for 2 hours at different pH value (2-8). It is observed from Fig. 6 that the removal efficiencies of Cu(II) increased with increasing pH and maximum adsorption of Cu(II) was obtained at pH 6.

At high pH, the precipitation of copper in aqueous solution was observed (Chang and Chen 2005). The effect of pH shows that sorption of Cu (II) is more favorable in acidic medium. At low pH values (acidic medium), imine and amine groups present in biguanide on surface of Fe<sub>3</sub>O<sub>4</sub>/m SiO<sub>2</sub>-Met nanoparticle, (Abu-El-Wafa *et al.*, 1987) protonated thus attract the number of places for chelating metal cations is reduced, resulting in positively charged due to the presence of the high concentration of H<sup>+</sup> ions.



**Fig. 6.** Effect of pH on the removal of Cu(II) using Fe<sub>3</sub>O<sub>4</sub>/mSiO<sub>2</sub>-Met.

**Effect of sorbent quantity.** Fig. 7 shows the removal of Cu(II) ions by Fe<sub>3</sub>O<sub>4</sub>/mSiO<sub>2</sub>-Met at different adsorbent doses (5-80 mg) for the 25 ml of Cu(II) solution (40 mg/l) at pH 6 ± 0.2 for 2 hours. Increase in adsorbent dosage increased the percent removal of ions, which is due to the increase in the number of active sites available in the adsorbent.

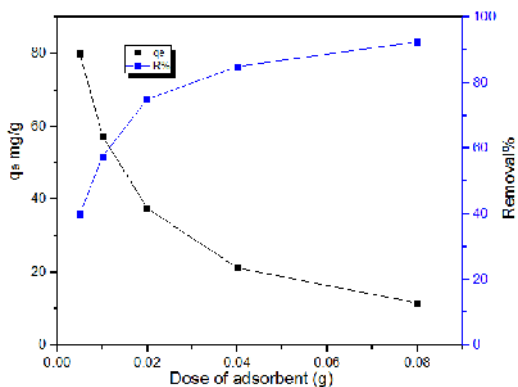


**Fig. 7.** Effect of dosage on the removal of Cu(II) using Fe<sub>3</sub>O<sub>4</sub>/mSiO<sub>2</sub>-Met

**Effect of contact time.** The effect of contact time on the adsorption of Cu(II) ions onto Fe<sub>3</sub>O<sub>4</sub>/mSiO<sub>2</sub>-Met nanoparticle for a fixed initial Cu(II) concentration, 40 mg/L and 20 mg of adsorbent at pH 6 ± 0.2 is shown in Fig. 8.

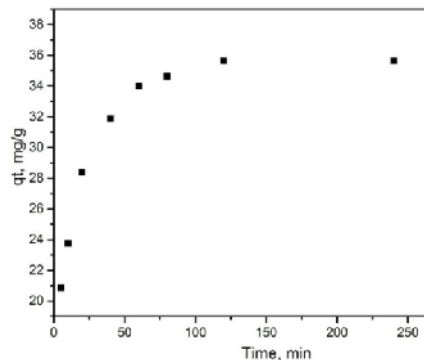


**Fig. 8.** Effect of contact time on the removal of copper (II) ion using Fe<sub>3</sub>O<sub>4</sub>/mSiO<sub>2</sub>-Met

**Effect of initial Cu(II) concentration.** The effect of the concentration of Cu(II) ions onto Fe<sub>3</sub>O<sub>4</sub>/mSiO<sub>2</sub>-Met nanoparticle was carried out by varying initial concentrations (C<sub>0</sub> Cu(II)) from 20 mg/L to 100 mg/L, pH = 6 ± 0.2. It is observed from Fig. 9. that the percentage removal of Cu (II) decreased from 90% to 40% by increasing the concentration from 20 mg/lit to 90 mg/lit respectively. This is because the sufficient adsorption sites are available at low initial concentration, but at higher concentrations due to the saturation of absorption by material self-absorption, decreased absorption efficiency.

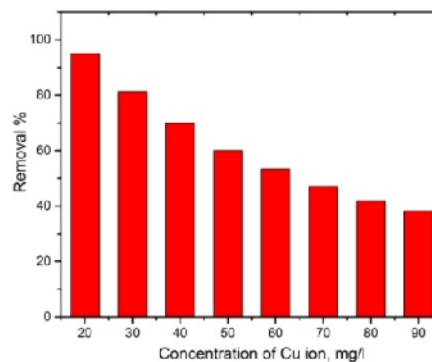


**Fig. 9.** Effect of Initial Concentration on the removal of Cu(II) using Fe<sub>3</sub>O<sub>4</sub>/mSiO<sub>2</sub>-Met.

**Adsorption model.** Langmuir (Eq. 1), Freundlich (Eq 2) isotherm were plotted by using standard straight line equation and corresponding two parameters for Cu(II) ion were calculated from their respective graphs.

$$\frac{1}{q_e} = \frac{1}{(q_{max}K_L)} \frac{1}{C_e} + \frac{1}{q_{max}} \quad \dots(1)$$

$$\ln q_i = \ln K_F + \frac{1}{n} \ln C_e \quad \dots(2)$$



$q_e$  is the amount of metal ions adsorbed per gram adsorbent (mg/g),  $C_e$  is the equilibrium concentration of metal ions (mg/l),  $q_{max}$  is the maximum adsorption of metal ions (mg/g) and  $K_L$  (l/mg) is the Langmuir adsorption equilibrium constant.  $K_F$  and  $1/n$  are the Freundlich constants related to adsorption capacity and adsorption intensity, respectively. The linearized Langmuir and Freundlich isotherm are obtained for copper ions and represented in (Figs 9, 10, Table 2).

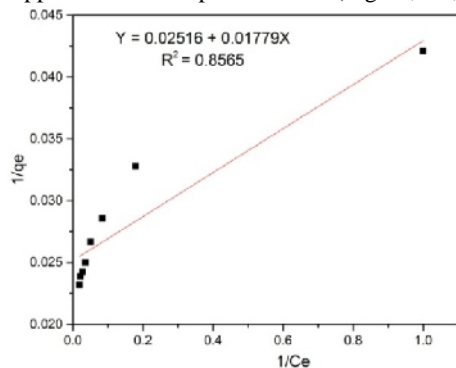


Fig. 9. Langmuir isotherm of adsorption of Cu(II) onto the Fe<sub>3</sub>O<sub>4</sub>/mSiO<sub>2</sub>-Met.

It is evident from comparing  $R^2$  values obtained from Langmuir and Freundlich plots that the experimental data perfect according to Freundlich isotherm ( $R^2 = 0.9963$ ). The slope of isotherm ( $1/n=0.15$ ), which was between 0 and 1, indicated the heterogeneity of the Fe<sub>3</sub>O<sub>4</sub>/mSiO<sub>2</sub>-Met nanoparticles (Mishra, Tiwari, Dubey and Mishra 1998) Furthermore, large  $K_F$  values (23.78) indicated that the magnetic nano-adsorbent had high adsorption capacity and high affinity for Cu(II) (Hirata, *et al.* 2002).

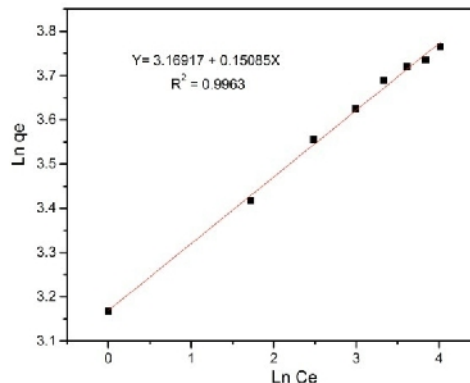


Fig. 10. Freundlich isotherm of adsorption of Cu(II) onto the Fe<sub>3</sub>O<sub>4</sub>/mSiO<sub>2</sub>-Met.

Table 2: Adsorption isotherm parameters for the Cu(II) onto the Fe<sub>3</sub>O<sub>4</sub>/mSiO<sub>2</sub>-Met.

| Metal  | Langmuir parameters |                  |       | Freundlich parameters |      |       |
|--------|---------------------|------------------|-------|-----------------------|------|-------|
|        | $K_L$ (L/mg)        | $q_{max}$ (mg/g) | $R^2$ | $K_F$ (L/mg)          | $n$  | $R^2$ |
| Cu(II) | 1.414               | 39.74            | 0.856 | 23.78                 | 6.63 | 0.996 |

**Desorption and reuse study.** In order to examine the possibility of regeneration and reuse of the Fe<sub>3</sub>O<sub>4</sub>/mSiO<sub>2</sub>-Met adsorbent, desorption experiments were studied by mixing 35 mg of adsorbent with 25 ml of Cu(II) solution (30 mg/l) for 2 hours at pH= 6.

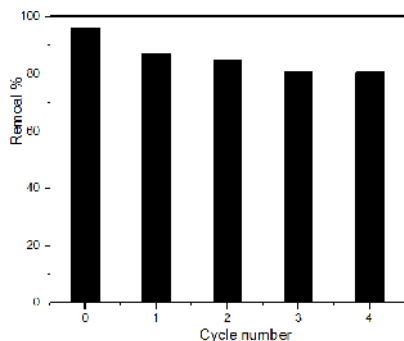


Fig. 11. Removal of Cu(II) using the regenerated Fe<sub>3</sub>O<sub>4</sub>/mSiO<sub>2</sub>-Met in different cycles.

Cu-loaded adsorbent was regenerated using 1 M HNO<sub>3</sub> solution and the regenerated adsorbent was reused in four consecutive cycles (Fig. 11).

**CONCLUSION**

In this study, a novel biguanide-functionalized mesoporous Fe<sub>3</sub>O<sub>4</sub>/mSiO<sub>2</sub>-Met nanoparticle was prepared for the adsorptive removal of Cu(II) from aqueous solutions. The equilibrium data of adsorption demonstrated good compatibility with Freundlich model. Furthermore, the magnetic adsorbent has large pore volume, superparamagnetism and active adsorptive sites that can be regenerated by simple washing with acid solution and separated from the reaction medium by the external magnetic field.

## REFERENCES

- Abu-El-Wafa, S., El-Ries, M., and Ahmed, F. (1987). "Formation of Metformin Complexes with Some Transition Metal Ions: Their Biological Activity," *Inorganica chimica acta*, **136**, 127-131.
- Ahmadi Nasab, N., Hassani Kumleh, H., Kazemzad, M., and Ghavipankeh, F. (2014). "Application of Spherical Mesoporous Silica Mcm-41 for Adsorption of Dibenzothiophene (a Sulfur Containing Compound) from Model Oil," *Iranian Journal of Chemistry and Chemical Engineering (IJCCE)*, **33**, 37-42.
- Alizadeh, A., Khodaei, M., Kordestani, D., Fallah, A., and Beygzadeh, M. (2012a). "The Successful Synthesis of Biguanide-Functionalized Mesoporous Silica Catalysts: Excellent Reactivity Combined with Facile Catalyst Recyclability," *Microporous and Mesoporous Materials*, **159**, 9-16.
- Alizadeh, A., Khodaei, M. M., Beygzadeh, M., Kordestani, D., and Feyzi, M. (2012b). "Biguanide-Functionalized Fe<sub>3</sub>O<sub>4</sub>/SiO<sub>2</sub> Magnetic Nanoparticles: An Efficient Heterogeneous Organosuperbase Catalyst for Various Organic Transformations in Aqueous Media," *Bulletin of the Korean Chemical Society*, **33**, 2546-2552.
- Ansari, F. B., Farooqui, M., and Quadri, S. (2010). "Complexation of Some Metal Ions with Metformin Hydrochloride in Acidic Aqueous Solutions," *Oriental Journal of Chemistry*, **26**, 667-670.
- Atia, A. A., Donia, A. M., and Shahin, A. E. (2005). "Studies on the Uptake Behavior of a Magnetic Co<sub>3</sub>O<sub>4</sub> Containing Resin for Ni (II), Cu (II) and Hg (II) from Their Aqueous Solutions," *Separation and purification technology*, **46**, 208-213.
- Beygzadeh, M., Alizadeh, A., Khodaei, M., and Kordestani, D. (2013). "Biguanide/Pd (Oac)<sub>2</sub> Immobilized on Magnetic Nanoparticle as a Recyclable Catalyst for the Heterogeneous Suzuki Reaction in Aqueous Media," *Catalysis Communications*, **32**, 86-91.
- Burleigh, M., Dai, S., Hagaman, E., and Lin, J. (2001). "Imprinted Polysilsesquioxanes for the Enhanced Recognition of Metal Ions," *Chemistry of materials*, **13**, 2537-2546.
- Chang, Y.C., Chang, S.W., and Chen, D.H. (2006). "Magnetic Chitosan Nanoparticles: Studies on Chitosan Binding and Adsorption of Co (II) Ions," *Reactive and Functional Polymers*, **66**, 335-341.
- Chang, Y.C., and Chen, D.H. (2005). "Preparation and Adsorption Properties of Monodisperse Chitosan-Bound Fe<sub>3</sub>O<sub>4</sub> Magnetic Nanoparticles for Removal of Cu (II) Ions," *Journal of colloid and interface science*, **283**, 446-451.
- De, M., Ghosh, P. S., and Rotello, V. M. (2008). "Applications of Nanoparticles in Biology," *Advanced Materials*, **20**, 4225-4241.
- Demirbas, A. (2008). "Heavy Metal Adsorption onto Agro-Based Waste Materials: A Review," *Journal of hazardous materials*, **157**, 220-229.
- Ghaemi, N., et al. (2015). "Polyethersulfone Membrane Enhanced with Iron Oxide Nanoparticles for Copper Removal from Water: Application of New Functionalized Fe<sub>3</sub>O<sub>4</sub> Nanoparticles," *Chemical Engineering Journal*, **263**, 101-112.
- Giri, S., Trewyn, B. G., Stellmaker, M. P., and Lin, V. S. Y. (2005). "Stimuli-Responsive Controlled-Release Delivery System Based on Mesoporous Silica Nanorods Capped with Magnetic Nanoparticles," *Angewandte Chemie*, **117**, 5166-5172.
- Gunasekaran, S., Natarajan, R., Renganayaki, V., and Natarajan, S. (2006). "Vibrational Spectra and Thermodynamic Analysis of Metformin," *Indian Journal of Pure and Applied Physics*, **44**, 495.
- Hasan, M., Selim, Y., and Mohamed, K. (2009). "Removal of Chromium Waste from Aqueous Waste Solution Using Liquid Emulsion Membrane," *Journal of hazardous materials*, **168**, 1537-1541.
- Hirata, M., et al. (2002). "Adsorption of Dyes onto Carbonaceous Materials Produced from Coffee Grounds by Microwave Treatment," *Journal of colloid and interface science*, **254**, 17-22.
- Järup, L. (2003). "Hazards of Heavy Metal Contamination," *British medical bulletin*, **68**, 167-182.
- Kresge, C., Leonowicz, M., Roth, W., Vartuli, J., and Beck, J. (1992). "Ordered Mesoporous Molecular Sieves Synthesized by a Liquid-Crystal Template Mechanism," *Nature*, **359**, 710-712.
- Li, G., Zhao, Z., Liu, J., and Jiang, G. (2011). "Effective Heavy Metal Removal from Aqueous Systems by Thiol Functionalized Magnetic Mesoporous Silica," *Journal of hazardous materials*, **192**, 277-283.
- Liu, J.F., Zhao, Z.S., and Jiang, G.B. (2008). "Coating Fe<sub>3</sub>O<sub>4</sub> Magnetic Nanoparticles with Humic Acid for High Efficient Removal of Heavy Metals in Water," *Environmental science & technology*, **42**, 6949-6954.
- Mishra, S. P., Tiwari, D., Dubey, R., and Mishra, M. (1998). "Biosorptive Behaviour of Casein for Zn<sup>2+</sup>, Hg<sup>2+</sup> and Cr<sup>3+</sup>: Effects of Physico-Chemical Treatments," *Bioresource technology*, **63**, 1-5.
- Ngah, W. W., Kamari, A., and Koay, Y. (2004). "Equilibrium and Kinetics Studies of Adsorption of Copper (II) on Chitosan and Chitosan/Pva Beads," *International Journal of Biological Macromolecules*, **34**, 155-161.
- Ngah, W. W., Teong, L., and Hanafiah, M. (2011). "Adsorption of Dyes and Heavy Metal Ions by Chitosan Composites: A Review," *Carbohydrate Polymers*, **83**, 1446-1456.
- Plazinski, W., and Rudzinski, W. (2009). "Modeling the Effect of Surface Heterogeneity in Equilibrium of Heavy Metal Ion Biosorption by Using the Ion Exchange Model," *Environmental science & technology*, **43**, 7465-7471.
- Ray, P. (1961). "Complex Compounds of Biguanides and Guanilyureas with Metallic Elements," *Chemical Reviews*, **61**, 313-359.
- Seprehian, H., Waqif-Husain, S., and Ghannadi-Maragheh, M. (2009). "Development of Thiol-Functionalized Mesoporous Silicate Mcm-41 as a Modified Sorbent and Its Use in Chromatographic Separation of Metal Ions from Aqueous Nuclear Waste," *Chromatographia*, **70**, 277-280.
- Vilensky, M. Y., Berkowitz, B., and Warshawsky, A. (2002). "In Situ Remediation of Groundwater Contaminated by Heavy-and Transition-Metal Ions by Selective Ion-Exchange Methods," *Environmental science & technology*, **36**, 1851-1855.
- Wang, J., et al. (2010). "Amino-Functionalized Fe<sub>3</sub>O<sub>4</sub>@ SiO<sub>2</sub> Core-Shell Magnetic Nanomaterial as a Novel Adsorbent for Aqueous Heavy Metals Removal," *Journal of colloid and interface science*, **349**, 293-299.
- Yang, D., Hu, J., and Fu, S. (2009). "Controlled Synthesis of Magnetite? Silica Nanocomposites Via a Seeded Sol-Gel Approach," *The Journal of Physical Chemistry C*, **113**, 7646-7651.
- Yu, B., Zhang, Y., Shukla, A., Shukla, S. S., and Dorris, K. L. (2000). "The Removal of Heavy Metal from Aqueous Solutions by Sawdust Adsorption-Removal of Copper," *Journal of hazardous materials*, **80**, 33-42.
- Zhu, M., Lu, L., Yang, P., and Jin, X. (2002). "Bis (1, 1-Dimethylbiguanido) Copper (II) Octahydrate," *Acta Crystallographica Section E: Structure Reports Online*, **58**, m217-m219.